CHAPTER 58

BRAGG REFLECTION OF WAVES BY ARTIFICIAL BARS

James T. Kirby[1], Jeffrey P. Anton[2]

Abstract

We consider the extension of previous theories for Bragg reflection of surface waves by parallel bars to the case of artificial bars placed discretely on the seabed. The case of non-resonant, weak reflection is considered first, followed by a consideration of the application of resonant interaction theory to the dominant Fourier mode of the bar field. Both theories are compared to numerical results, and discrepancies are seen in both cases. Finally, experimental results are compared to theory.

Introduction

The discovery that the Bragg reflection mechanism leads to strong reflection of incident surface waves by periodic bottom undulations has led to speculation that artificial bars could be constructed which would partially shelter shores or localized structures from wave attack. Possible bar configurations of this sort have been discussed previously by Mei et al. (1988) and Naciri and Mei (1988). The paper by Bailard et al. (1990) in this conference describes an effort which was made to install and test an artificial bar field offshore of a natural beach.

The purpose of the present study was to extend the scope of available theory and techniques which were available for predicting wave reflection from bars, in support of the proposed field study. Here, we discuss the application of analytic perturbation methods for both non-resonant and resonant cases. We also discuss numerical results, which point out limitations present in both analytic approaches. Finally, experimental results largely provide a qualitative verification but in turn show some limitation of the small amplitude bar theory.

Theory for Small Amplitude Bars

The theory which provides the framework for analysis here is given by an extended mild-slope equation derived by Kirby (1986).

We treat the water depth $h'(x,y)$ as the superposition of a mildly-sloping bottom $h(x,y)$ and a rapidly-varying but small- amplitude undulation $\delta(x,y)$:

$$h'(x,y) = h(x,y) - \delta(x,y) \tag{1}$$

[1]Assoc. Prof., Center for Applied Coastal Research, Dept. of Civil Engrg., Univ. of Delaware, Newark, DE 19716

[2]Formerly, Grad. Stud., Coastal and Oceanographic Engineering Department, University of Florida, Gainesville, FL 32611

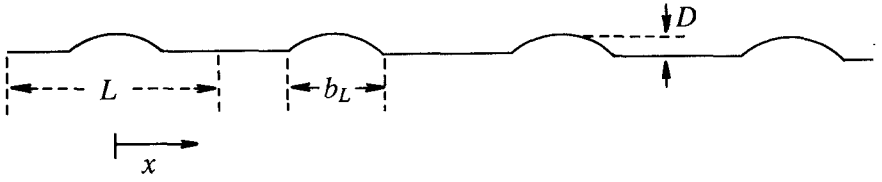

Figure 1: Bar field with four discrete bars.

Using $h(x,y)$ as the reference depth in the mild-slope sense, the model equation

$$\nabla_h \cdot (CC_g \nabla_h \phi) + k^2 CC_g \phi = \frac{g}{\cosh^2 kh} \nabla_h \cdot (\delta \nabla_h \phi) = 0 \tag{2}$$

is obtained, where ϕ is the value of the linear wave potential at the still water surface. The model coefficients are obtained from

$$\omega^2 = gk \tanh kh \; ; \; C = \frac{\omega}{k} \; ; \; C_g = \frac{\partial \omega}{\partial k} \tag{3}$$

and are determined by the value of $h(x,y)$ in all cases.

The Artificial Bar Field

In the absence of appropriate field data, we have restricted our attention here to the study of periodically spaced bars ($\delta = \delta(x)$) and an otherwise uniform depth h = constant. In principal, δ is arbitrary aside from the small amplitude restriction. In the present study, we have chosen a bottom consisting of rectified sine waves, given by

$$\delta(x) = \begin{cases} D \cos \frac{\pi}{b_L}(x - NL) \; ; & NL - \frac{b_L}{2} \leq x \leq NL + \frac{b_L}{2} \\ 0 & \text{otherwise} \end{cases} \tag{4}$$
$$N = 0, \ldots, N_b - 1$$

where N_b is the number of bars, L is the periodic bar spacing, b_L is the footprint of the bar on the bottom, and D is the bar height. The rectified cosine form is chosen mainly for its convenience in later analysis. An example bar field is shown in Figure 1. The bar field is periodic over intervals of width L, and can be conveniently represented by the cosine series,

$$\delta(x) = \sum_{n=0}^{\infty} D_n \cos(n\lambda x) \quad ; \quad \lambda = \frac{2\pi}{L} \tag{5}$$

where

$$D_0 = \frac{D}{\pi} \; ; \; D_1 = -\frac{D}{2} \; ; \; D_n = D \frac{\cos\left(\frac{n\pi}{2}\right)}{\pi(1 - n^2)} (1 + \cos n\pi) \tag{6}$$

Non-resonant Reflection

For the case of h constant, the model equation (2) may be written as

$$\nabla_h^2\phi + k^2\phi = \alpha\nabla_h \cdot (\delta\nabla_h\phi) \tag{7}$$

where

$$\alpha = \frac{4k}{2kh + \sinh 2kh} \tag{8}$$

With $\delta(x)$ representing bars varying in the x-direction, we represent oblique waves according to

$$\phi(x,y) = \tilde{\phi}(x)e^{imy} \; ; \; m = k\sin\theta \tag{9}$$

and obtain

$$\begin{aligned} \tilde{\phi}_{xx} + \ell^2\tilde{\phi} &= \alpha(\delta\tilde{\phi}_x)_x - m^2\alpha\delta\tilde{\phi}\,, \\ \ell^2 &= k^2 - m^2 = k^2\cos^2\theta \end{aligned} \tag{10}$$

This equation has been obtained by Miles (1981) who used it to study reflection from a single isolated obstacle.

For $\delta(x)$ confined in a finite region of space, we may write

$$\begin{aligned} \tilde{\phi}(x \to \infty) &= Te^{i\ell x} \\ \tilde{\phi}(x \to -\infty) &= e^{i\ell x} + Re^{-i\ell x} \end{aligned} \tag{11}$$

where T and R are complex transmission and reflection coefficients. With δ small, we expand $\tilde{\phi}$, T and R as series in the small parameter $\epsilon = D/h$, and obtain

$$\phi_0 = e^{i\ell x} \qquad R_0 = 0 \qquad T_0 = 1 \tag{12}$$

at leading order. At second order, the reflection coefficient R_1 for an arbitrary topography $\delta(x)$ is

$$R_1 = -\frac{i\alpha}{2\ell}\left(\ell^2 - m^2\right)\int_{-\infty}^{\infty}\delta(x)e^{2i\ell x}dx \tag{13}$$

as found by Miles (1981). Note that R_1 is singular in the limit as $\theta \to \pi/2$. This effect has not been previously noted and its practical implications are unclear.

For the case of a simple sinusoidal bottom

$$\delta(x) = D\sin(\lambda x) \; ; \; 0 \le x \le N_b L \tag{14}$$

we obtain the expression

$$|\,R\,| = \begin{cases} \frac{\alpha D}{2}\left(\frac{\ell^2-m^2}{\ell^2}\right)\frac{2\ell/\lambda}{\frac{2\ell}{\lambda}^2-1}\left|\sin\left(\frac{2\ell}{\lambda}\pi N_b\right)\right| \; ; \; \frac{2\ell}{\lambda} \neq 1 \\ \frac{\alpha D}{2}\frac{(\ell^2-m^2)}{\ell^2}\frac{\pi N_b}{2} \; ; \; \frac{2\ell}{\lambda} = 1 \end{cases} \tag{15}$$

This result extends the non-resonant theory of Davies and Heathershaw (1984) to include obliquely incident waves.

For the periodic bar field described by (5) and (6), we substitute (5) in (13) and obtain the expression

$$R_1 = \frac{-i\alpha}{2}\left(\frac{\ell^2 - m^2}{\ell}\right)\sum_{n=0}^{\infty} D_n I_n \ , \tag{16}$$

where the integrals I_n are given by

$$I_n = \int_{-\frac{L}{2}}^{(N_b-1)L+\frac{L}{2}} \cos(n\lambda x) e^{2i\ell x} dx. \tag{17}$$

As in the case of a single sinusoidal bar, the integral I_n takes on special values when $2\ell/n\lambda = 1$ for the corresponding value of n. We further simplify the notation by setting

$$\gamma = \frac{2\ell}{\lambda} \tag{18}$$

Then, for $\gamma \neq n$, we obtain the expression

$$I_n(\gamma) = \frac{\gamma^2}{\ell(\gamma^2 - n^2)} e^{i\ell N_b L} \sin \ell N_b L \ ; \ \gamma \neq n \tag{19}$$

For $n = \gamma$, we obtain the expression

$$I_n(\gamma = n) = \frac{N_b L}{2} \tag{20}$$

We thus obtain the general solution for obliquely incident waves

$$R_1 = -\frac{i\alpha}{2}\left(\frac{\ell^2 - m^2}{\ell^2}\right)\left\{\sum_{n=0,\gamma\neq n}^{\infty} \frac{\gamma^2 D_n}{(\gamma^2 - n^2)} e^{i\ell N_b L} \sin \ell N_b L + D_n \delta(n-\gamma)\frac{\ell N_b L}{2}\right\} \tag{21}$$

where $\delta(n-\gamma)$ is the delta function, and there $n = \gamma$ can only occur for one wavenumber component for a fixed value of ℓ. For the case of normally incident waves (studied further below), we let $\ell \to k$, $m \to 0$ and obtain

$$R_1 = -\frac{i\alpha}{2}\left\{\sum_{n=0}^{\infty} \frac{\gamma^2 D_n}{(\gamma^2 - n^2)} e^{ikN_b L} \sin kN_b L + D_n \delta(n-\gamma)\frac{kN_b L}{2}\right\} \tag{22}$$

From the form of the solution, it is apparent that each harmonic of the bar field contributes to the reflection process, with the dominant contribution of the n^{th} harmonic coming from the neighborhood $\lambda \approx n$. An example plot of reflection coefficient $|\ R_1\ |$ is shown in Figure 2 for a case of 4 bars with crest-to-crest spacing equal to the unrectified wavelength ($b_L = L/2$). Waves are normally incident on the bar field. The peak in $|\ R_1\ |$ at $2k/\lambda = 1$ corresponds to the usual Bragg interaction between the surface wave and the fundamental harmonic of the bar field, when the surface wave length is twice the bar spacing. A second prominent peak is located at $2k/\lambda = 2$, corresponding to a surface wavelength equal to twice the length of the second harmonic of the bar field (and thus equal in length to the bar spacing). This strong second peak is absent when the bar

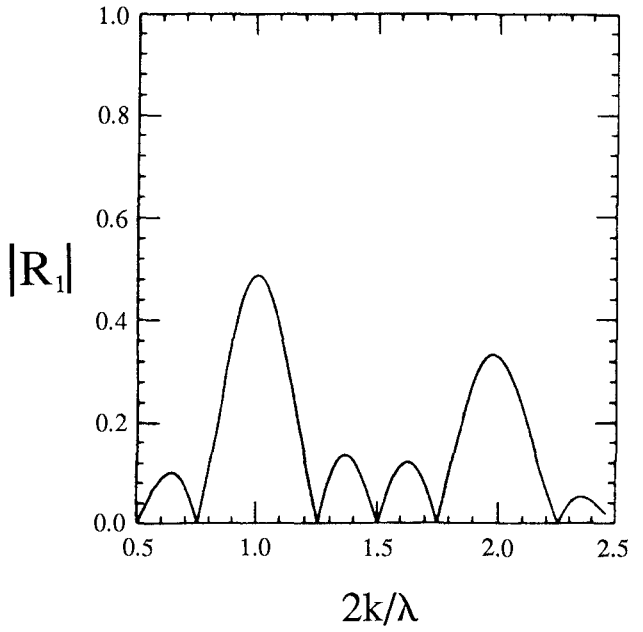

Figure 2: Reflection for four discretely placed bars. Non-resonant theory, equation (22).

field being considered is a simple sinusoid, as in Davies and Heathershaw (1984) and Mei (1985).

In general, the relative amplitude of the peaks in the reflection coefficient may be adjusted by changing the spacing of artificial bars, assuming the cross-section of each bar to stay the same. Pushing bars closer together makes the bar field more sinusoidal and reduces the importance of higher harmonics. Placing the bars further apart makes them into relatively more "solitary" features, and thus emphasizes the relative importance of higher harmonics. Two cases illustrating these extremes were investigated in the experiments described below.

Resonant Reflection

The reflection coefficient described in (21) is defective for the cases $2\ell \approx n\lambda$, where the coefficient can become arbitrarily large as $N_b \rightarrow \infty$. While this limit would never be reached in practice, the result shows that the theory is not strictly valid in the neighborhood of the resonances. The problem lies with assuming that R_1 is $< O(1)$ in the perturbation series used above. Mei (1985) has developed a resonance theory which allows for $O(1)$ reflection in the neighborhood of each resonance. Mei et al. (1988) further suggested that, for the case of a bar field with multiple Fourier components, the reflection could be estimated using the resonance theory applied to the Fourier mode corresponding to the bar wavelength. This approach would not account for the occurrence of multiple strong peaks. In the present study, we define a neighborhood of each resonance $2\ell/\lambda = n$ to be the range $n - 1/2 \leq 2\ell/\lambda \leq n + 1/2$. Then, in each range, Mei's theory is used with $2\ell/\lambda^*$ replacing $2\ell/\lambda$, with $\lambda^* = n\lambda$. We refer the reader to Mei (1985) for the expressions defining the reflection coefficients. The only necessary modification to the theory account for oblique incidence and the presence of multiple resonant peaks. The frequency ω_n of the n^{th} resonant peak is given by

$$\omega_n^2 = \frac{gn\lambda}{2\cos\theta} \tanh\left(\frac{n\lambda h}{2\cos\theta}\right) \tag{23}$$

The cutoff condition Ω_0 defined by Mei is replaced by

$$\Omega_{0n} = \frac{\ell^2 - m^2}{\ell^2} \frac{\omega_n k D_n}{2\sinh 2kh} \quad ; \quad k = \frac{\ell}{\cos\theta} \tag{24}$$

where the D_n are the amplitudes of the bar Fourier coefficients, and there Ω_{0n} refers to the n^{th} resonant peak.

An example of the reflection calculated for the case of normal incidence is given in the following section, in comparison with numerical results and results of the non-resonant theory.

Numerical Solutions

In order to study the validity of each of the perturbation solutions, direct numerical solutions of equation (10) were also performed. For a bar field in the region $0 \leq x \leq N_b L$, an incident wave boundary is established at $x = A < 0$, and a downwave, transmitting boundary is established at $x = B > N_b L$. For an incident wave $\tilde{\phi}_I = e^{i\ell x}$, the appropriate boundary conditions are

$$\tilde{\phi}_x = \begin{cases} i\ell(2\tilde{\phi}_I - \tilde{\phi}) \,; & x = A \\ i\ell\tilde{\phi} \,; & x = B \end{cases} \tag{25}$$

Equations (10) and (25) are finite-differenced using central differences, leading to a tridiagonal system which is solved using the Thomas algorithm.

Figure 3 shows a sample of calculated reflection coefficients obtained with the numerical solution and the two analytic solutions, for the bar field described in Figure 2. As expected, the non-resonant solution over-predicts reflection at $2k/\lambda = 1$, in comparison with the resonant theory of Mei (1985). The discrepancy is relatively minor at the second peak $2k/\lambda = 2$, where the resonance is relatively weaker. In contrast to both analytic theories, the numerical results

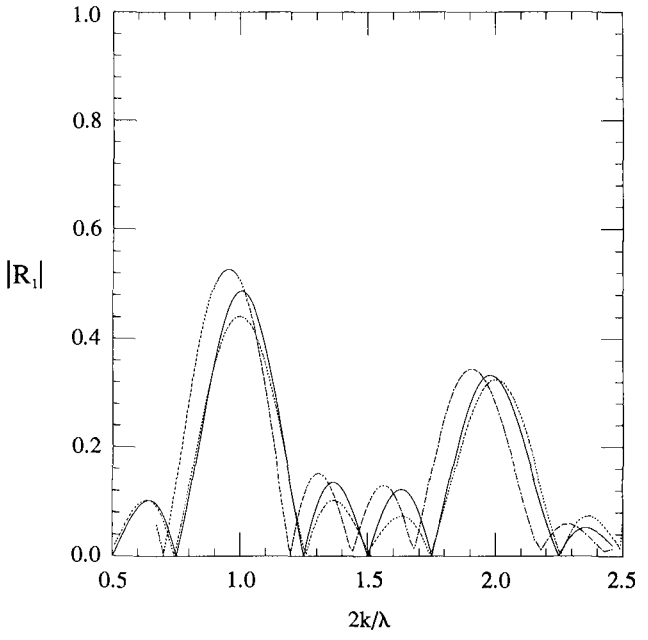

Figure 3: Comparison of non-resonant, resonant and numerical solutions for a bar field with $N_b = 4$. ———, non-resonant theory; – – ––, resonant theory; — · —, numerical results.

show a strong downshift of the reflection peaks to lower values of $2k/\lambda$. This downshift is related to the simultaneous interaction between the wave field and several bottom modes; a similar effect occurs for the case of a sinusoidal bar field, but it is much more subtle. The numerical scheme also predicts a higher reflection coefficient at each peak. The large downshifts and higher peaks are largely validated by data described below. These results indicate that either of the two analytic solutions are at best qualitatively accurate when used to describe reflection from the type of bars that could be built in an actual construction project.

Experimental Results

Experiments were conducted in the 60 cm wide wave flume in the Coastal and Oceanographic Engineering Laboratory, University of Florida, in order to verify the basic aspects of the theory for normally incident waves. For the experiments, a water depth $h = 15\ cm$ was used. Bar height D was 5 cm, giving $D/h = 0.33$, which is relatively large and could contribute to some of the discrepancies between theory and data noted below. The bar footprint $b_L = 50cm$. Two bar spacings, $L = 80cm$ and $120cm$, were tested, corresponding to cases with bar field higher harmonics of low importance and great importance,

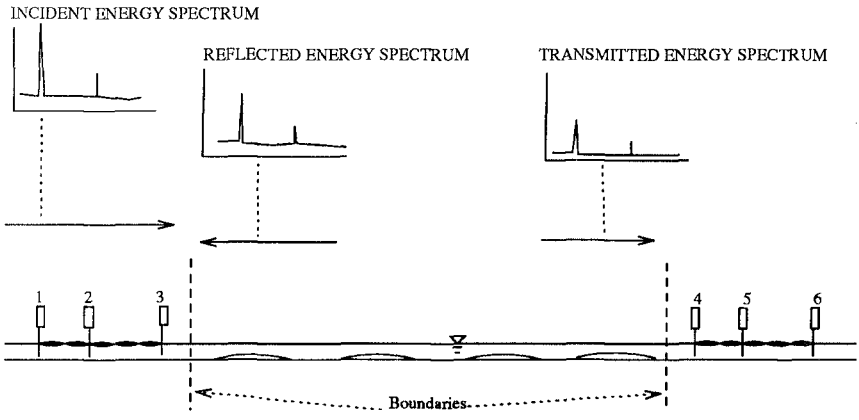

Figure 4: Bar field and wave gage placement

respectively. The bar fields tested contained four discrete bars.

In order to maintain a close correspondence between the assumed linearity of the wave theory and the experiments, incident waves on the order of 1 cm in height were generated. (Actual height varied with wave frequency, as would be expected from wavemaker theory.) Wave heights were measured using capacitance wave gages mounted with 6 cm-long wires, which were calibrated over their full length. Data was sampled using 12-bit digitization, giving a resolution of 0.012 mm/division. The wavefield was sampled at a $10Hz$ frequency, with experimental waves being generated in the range $0.4Hz \leq f \leq 1.6Hz$.

Due to the small wave heights being used, there was an additional source of noise in the data associated with mechanical vibration in the wavemaker and other high-frequency effects. In retrospect, it would be better to use slightly higher waves in future experiments unless great care were taken to isolate mechanical vibration. (For a particularly spectacular example of clean data in a related low-amplitude wave experiment, see Benjamin et al. (1989)).

The three-gage, least squares method developed by Funke and Mansard (1980) was used to separate incident and reflected waves. The gage layout relative to the bar field is shown in Figure 4. The incident-reflected separation was performed both upwave and downwave of the experimental bar field. The downwave separation indicated a reflection from the absorbing beach on the order of 5–6%. This reflected energy was neglected in subsequent processing and the downwave region was assumed to be perfectly transmitting.

Figure 5 shows the measured reflection coefficient for the case of $L = 80cm$, when bar field harmonics are relatively unimportant. Also included in the figure is the prediction of the numerical model described in the previous section. The data largely validates the theory, although there is a great deal of scatter. (It also appears that shifting the data to higher values of $2k/\lambda$ would bring the data into fairly close agreement with theory. No systematic error was ever detected in the experimental procedure which could account for such a shift, unfortunately.)

Figure 6 shows corresponding data for the case of $L = 120cm$, where the

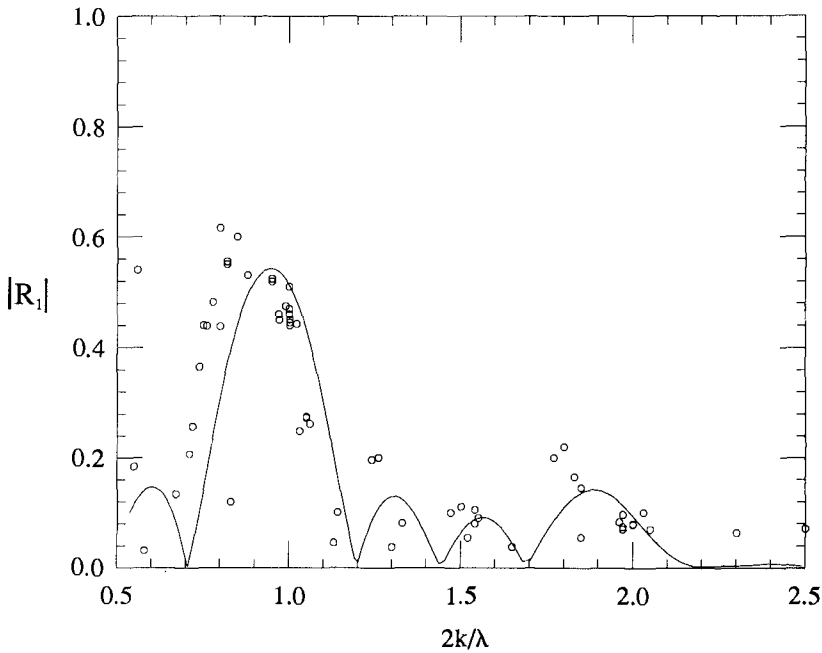

Figure 5: Experimentally measured reflection coefficient, $L = 80cm$.

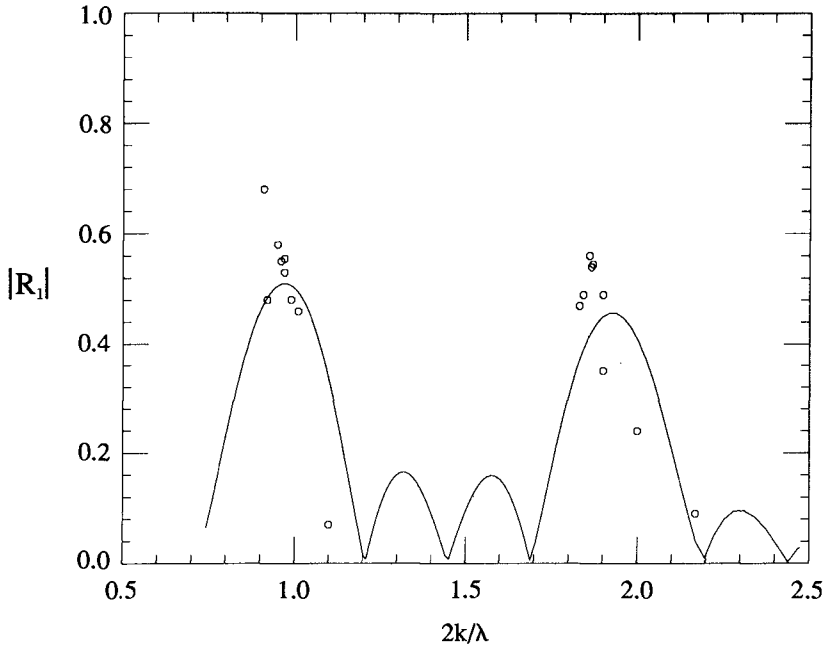

Figure 6: Experimentally measured reflection coefficient, $L = 120cm$.

second harmonic component of the bar field is comparable in height to the fundamental harmonic. Due to time constraints, the data here is relatively sparse, and tests were grouped in order to show the relative heights of the two reflection peaks. Both the presence and the relative importance of the two numerically-predicted peaks are substantiated by the data.

Response of a Closed-end Channel

One question that arises in response to the realization that bars can reflect significant amounts of incident energy is whether or not a region downwave of a bar field experiences a less severe wave condition than the region on the incident site. The answer to this question can be positive or negative, depending on the geometry of the downwave region and the reflectivity of the end boundary. For cases where reflection from the end wall is nearly complete, waves travelling back towards the bar field are partially re-reflected into the sheltered region. The possibility of resonating the sheltered region exists, as does the possibility of reducing the wave activity, and depends primarily on whether the sheltered region contains an integer multiple of one-half the surface wavelength.

Figure 7 shows the numerically predicted amplitude at a vertical wall situated four barfield wavelengths downwave of a bar field with four bars, as in the previous examples. The incident wave has an amplitude of unity, and so an amplitude of 2 represents simple reflection. The figure shows that the amplitude at the wall can reach as high as 3.6 and as low as 1, representing a range of

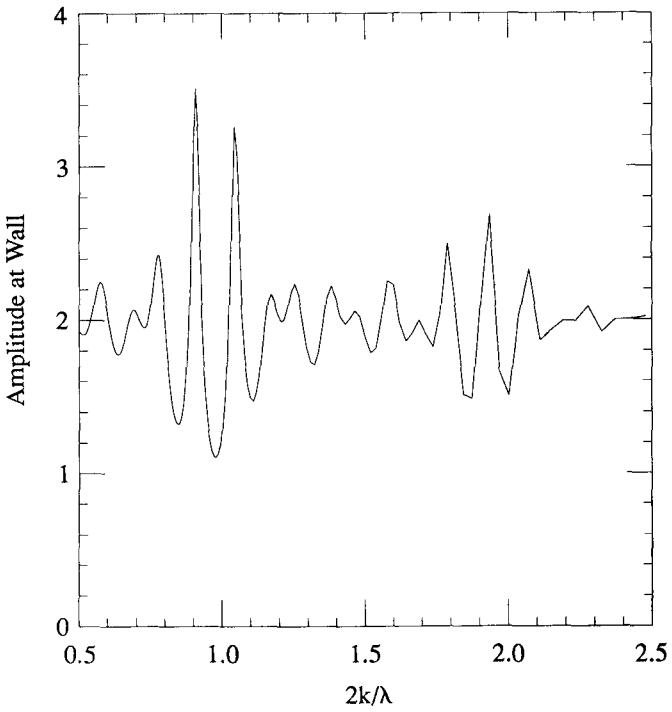

Figure 7: Wave Amplitude at End Wall of a Channel Sheltered by an Artificial Bar Field

resonance and sheltering conditions.

For the case where the channel end is primarily absorbing (due to wave breaking or frictional effects), the possibility of resonating the sheltered region is greatly reduced. This virtually guarantees that a bar field designed to shelter a beach from wind-wave band waves would not resonate the shoreline. However, as the wave frequency becomes low, even a mildly-sloped shoreline can become essentially reflective. It is thus possible that broad, low bars contribute significantly to amplifying long wave energy on the beach face. The long waves that could be amplified or resonated by this mechanism may be locally generated by nonlinear processes in the surfzone, or they may be arriving as part of the forced or free long wave climate incident from offshore. Problems of this sort need further investigation to determine the relative importance of bottom interaction in influencing the nearshore wave climate.

Acknowledgements

The work described in this paper was supported by the Office of Naval Research and the Naval Civil Engineering Laboratory through contracts N00014-86-K-0790 and N00014-89-J-1717. Both authors were affiliated with the Coastal and Oceanographic Engineering Department, University of Florida at the start of this study; use of the facilities there is greatly appreciated. Conversations with Jim Bailard, Bob Guza, and Dan Hanes were instrumental in the early stages of problem formulation.

References

Baillard, J., DeVries, J., Kirby, J.T. and Guza, R.T., 1990, "Bragg reflection bars: A new shore protection concept?" *Proc. 21st Int'l. Conf. Coastal Engrg.*

Benjamin, T.B., Boczar-Karakiewicz, B. and Pritchard, W.G., 1987, "Reflection of water waves in a channel with corrugated bed," *Journal of Fluid Mechanics*, 185, 249-274.

Davies, A.G. and Heathershaw, A.D., 1984, "Surface-wave propagation over sinusoidally varying topography," *Journal of Fluid Mechanics*, 144, 419-433.

Funke, E.R. and Mansard, E.P.D., 1980, "Measurement of incident and reflected spectra using a least squares approach," *Proc. 17th Int'l. Conf. Coastal Engrg.*, 1, 154-172.

Kirby, J.T., 1986, "A general wave equation for waves over rippled beds," *Journal of Fluid Mechanics*, 162, 171-186.

Mei, C.C., 1985, "Resonant reflection of surface water waves by periodic sandbars," *Journal of Fluid Mechanics*, 152, 315-335.

Mei, C.C., Hara, T. and Naciri, M., 1988, "Note on Bragg scattering of water waves by parallel bars on the seabed," *Journal of Fluid Mechanics*, 186, 147-162.

Miles, J.W., 1981, "Oblique surface-wave diffraction by a cylindrical obstacle," *Dynamics of Atmospheres and Oceans*, 6, 121-123.

Naciri, M. and Mei, C.C., 1988, "Bragg scattering of water waves by a doubly periodic seabed," *Journal of Fluid Mechanics*, 192, 51-74.